Identification of Topological Constraints in Entangled Polymer Melts Using the Bond-Fluctuation Model

Sachin Shanbhag* and Ronald G. Larson

Department of Chemical Engineering, University of Michigan, Ann Arbor, Michigan 48109-2136

Received October 27, 2005; Revised Manuscript Received January 15, 2006

ABSTRACT: We propose an algorithm to locate individual entanglements along chains, equilibrated using the bond-fluctuation lattice model. The algorithm identifies entanglements as local deviations of the primitive path from the shortest possible path between beads on a chain that are on lattice sites. For well-entangled chains (number of beads, $N \geq 125$), the average number of entanglements enumerated using the proposed method is in excellent agreement with the number of entanglements per chain inferred using the ensemble-averaged primitive path length $\langle L_{pp} \rangle$ and mean-squared end-to-end distance $\langle R^2 \rangle$ of the chains, namely $Z = \langle L_{pp} \rangle^2 / \langle R^2 \rangle$. As an application of this method, we show that the elimination of an entanglement releases, approximately, one additional entanglement. This implies a value of $\alpha = 1.03 \pm 0.02$ for the "dilution exponent" relating entanglement density ρ_{ent} to polymer concentration c via $\rho_{ent} \propto c^{1+\alpha}$ and is consistent with the description of entanglements as binary contacts.

Introduction

Viscoelastic properties of linear polymer melts depend sensitively on the chain length, and the dynamics of long chains are controlled by entanglements which arise due to topological interactions between chains. Since entanglements are not directly observable via experiments, computer simulation is an important tool to understand their nature. Indeed, several investigators, including Kremer, Grest, and co-workers in particular, have shed significant light on the role of entanglements in governing the relaxation modulus of polymer melts via molecular dynamics simulations.[1−7]

For highly entangled polymer melts, the equilibration or longest relaxation time at room temperature is typically beyond the range of time scales readily accessible by standard molecular dynamics schemes.[8] One possible recourse is to use coarse-grained lattice Monte Carlo methods such as the bond-fluctuation model (BFM), introduced by Carmesin and Kremer and modified by Shaffer to model highly entangled polymer systems.[9,10] The primary advantage of Shaffer's modification (referred to henceforth as S-BFM)[10] over the original bond-fluctuation model is that with the former a chain-crossing event that violates topological restrictions can be recognized easily. When such chain-crossing events are permitted in dense systems (fractional occupancy $\phi \sim 0.5$), the chains reproduce Rouse dynamics, and when such events are forbidden for long chains, they reproduce reptation dynamics.[10] This S-BFM has therefore been used to study the role of chain topology in the transition from Rouse to reptation dynamics,[11] structure and dynamics of polymer melts in confined geometries,[12] the persistence of interchain contacts in entangled and unentangled melts,[13] the self-diffusion of mildly entangled star molecules in melts and in solutions of varying concentrations,[14,15] and the chain-retraction potential in entangled polymers.[16]

Although well-entangled polymer melts can be simulated using S-BFM, only ensemble-averaged properties, such as the average number of primitive path (PP) steps per chain, have been computed.[10,11,16] Off-lattice methods to specify the number and location of "topological obstacles" that a particular chain in the ensemble has to navigate around have been suggested;[7,18] however, no such method exists for treating lattice models.[17] In this article we propose a new algorithm to determine the spatial position of entanglements or constraints along individual chains with S-BFM. As an application, we use this algorithm to investigate the nature of coupling between entanglements by raising the following question: how many additional entanglements are released when a chain i in a polymer melt with Z_i entanglements is removed?

The next section presents a description of the model and introduces the algorithm used to enumerate entanglements. In the following section, we validate the algorithm and use it to investigate topological coupling between PPs.

Model and Method

Beads that make up polymer chains are placed as self-avoiding random walks on a regular 3D cubic lattice. BFM gets its name from the fact that the length of the bond or vector, **b**, connecting successive beads along a chain, fluctuates over a significant range. For the 2D lattices considered by Carmesin and Kramer,[9] $2 \leq |\mathbf{b}| \leq \sqrt{13}$, in units of lattice spacing. A modification to the original scheme, implemented by Shaffer for 3D lattices,[10−12] narrows the set of permitted bond lengths to $|\mathbf{b}| \in \{1, \sqrt{2}, \sqrt{3}\}$. This choice of acceptable values of $|\mathbf{b}|$ confers three primary advantages by exploiting the geometry of the lattice:

1. By forbidding moves in which the midpoints of bonds intersect, topological constraints can easily be enforced. Thus, S-BFM is suitable for examining spatial restrictions in concentrated systems or melts, where entanglement effects dominate.

2. Compared with bead−spring molecular dynamics simulations, S-BFM results in a relatively low number of monomers per entanglement, N_e. Typically, $N_e \approx 30$,[16] which allows for well-entangled systems (large N/N_e) to be simulated.

3. Bond crossing can be permitted or forbidden. There is no change in static properties when bonds are allowed to pass through each other. However, the dynamics are speeded up, and the computational load to equilibrate a melt is substantially reduced.

Equilibration. A bead density of $\phi = 0.5$ in the BFM has been found to be adequate to describe polymer melts.[10,14,16,19] To grow chains on the lattice, we initially execute self-avoiding

10.1021/ma052317v CCC: $33.50
Published on Web 02/07/2006

random walks, selecting bond types $\{1, \sqrt{2}, \sqrt{3}\}$ with probabilities {3/13, 6/13, 4/13}, respectively.

Excluded-volume interactions between beads are imposed by disallowing multiple occupancy of lattice sites. *Chain connectivity* is enforced by confining the fluctuation of the bond length to the set $\{1, \sqrt{2}, \sqrt{3}\}$. *Chain uncrossability* is switched on (off) by prohibiting (permitting) moves that lead to configurations in which the midpoints of bonds intersect. In a trial move a randomly chosen bead is displaced by one lattice unit. The move is accepted if it does not violate the excluded volume, chain connectivity, and chain uncrossability criteria.

During the first phase of equilibration, chains are allowed to cross each other to facilitate rapid equilibration of the interior portions of chains (on time scales much shorter than reptation time). As mentioned before, the global structural features of crossing and noncrossing chains are indistinguishable. In the second phase of equilibration, chain crossing is turned off. We examined the decay of the end-to-end autocorrelation vector, $\langle \mathbf{P}(t) \rangle = \langle \mathbf{R}(t) \cdot \mathbf{R}(0) \rangle / \langle R^2(0) \rangle$. In the first phase, $1.0 \geq \langle \mathbf{P}(t) \rangle \geq 0.3$, chain crossing is allowed, whereas in the second phase, $0.30 \geq \langle \mathbf{P}(t) \rangle \geq 0.05$, it is disallowed.

Annealing and the Primitve Path Network. Shanbhag and Larson reformulated,[16] for lattice simulations, the annealing algorithm proposed by Everaers et al. to compute the primitive paths (PP) of equilibrated chains.[6] Note that the term "annealing" here does not refer to a decrease in temperature; rather, it denotes an artificial process in which beads are allowed to overlap, thus decreasing the contour length of the chain, while steadily decreasing the tolerance with which moves that increase the contour length again are accepted. The intent is to allow chains slowly to shrink their length while maintaining their noncrossability with other chains, until all chains have collapsed onto paths of minimum total length that preserve their original topological interactions. These shrunken chain contours are identified as the PPs. In the annealing algorithm, the end beads of all the equilibrated chains are immobilized while the interior beads are unrestrained and allowed to move. Intramolecular excluded-volume effects are turned off while maintaining intermolecular excluded-volume interactions and chains in the system are annealed simultaneously;[6,16] i.e., the acceptance probability is gradually reduced according to the expression

$$p_{\mathrm{acc}}(t) = \exp\left[-A\Delta L\left(\frac{t}{\tau_{\mathrm{anneal}}}\right)^2\right] \tag{1}$$

where ΔL is the change in contour length due to the trial move. In our simulations, we set $A = 16$ and $\tau_{\mathrm{anneal}} = 10\tau_{\mathrm{Rouse}}$, where τ_{Rouse} is the Rouse relaxation time. This choice implies that $p_{\mathrm{acc}} = 1/e$ when $t/\tau_{\mathrm{anneal}} = 1/4$ for $\Delta L = +1$. As reported previously,[16] the ensemble averages are insensitive to the details of the function assumed for p_{acc}. For example, increasing τ_{anneal}, which controls the period of "cooling", or varying A, which controls the rate of cooling, within the range 10−20 yields indistinguishable results. Initially, during the annealing operation, most of the moves that do not violate toplogical restrictions are accepted. As the system "cools", moves that decrease the total contour length are preferentially accepted, and the chain contours contract to their PPs. Since intrachain excluded volume is disabled, the annealing algorithm ignores chain self-entanglements. However, Sukumaran et al.[7] varied the degree of intrachain excluded-volume interactions and found that the contribution of self-entanglements is negligible.

In the limit of fast cooling $A \rightarrow \infty$

$$p_{\mathrm{acc}} = \begin{cases} 0 & \text{if } \Delta L > 0; \\ 1 & \text{if } \Delta L \leq 0 \end{cases} \tag{2}$$

We label this limit, in which only moves that strictly decrease the contour length are accepted, as "quenching".

In this paper we adopt the method of Shanbhag and Larson,[16] in which the total *length* of the chains in the system is minimized to obtain PPs. In the molecular dynamics (MD) simulation of Everaers et al. the total *energy* of the system was minimized.[6] Using a MD formulation, Zhou and Larson analyzed the difference between the two minimization procedures to obtain PPs. They found that the average PP lengths obtained by minimization of length[16] and energy[6] of an equilibrated ensemble are essentially identical.[20] However, the distribution of the PP lengths obtained via energy minimization is narrower than that obtained from length minimization. Further, the distribution of PP lengths obtained by their simulations was in excellent agreement with the results from lattice simulations when length minimization was adopted to anneal the equilibrated chains to their PPs.[20] It may also be noted that the geometrical algorithm recently developed by Kröger,[18,21] inherently minimizes the total length of the chains.

Enumerating Entanglements. The PP of an unentangled chain is a straight line connecting its ends. In an entangled system of chains, the chain has to navigate around obstacles, and the PP becomes tortuous. Thus, the increase in the length of the PP over that of a straight path connecting the same two ends is a measure of the number of obstacles in its trajectory. To identify the spatial location of individual entanglements, the local structure of the PP has to be inspected. Therefore, we seek the smallest element of the PP that can be examined for deviations from the shortest path. The distance between neighboring beads is always a straight line connecting them and cannot be used. Thus, we conjecture that if the trajectory of the PP between a "bead" and its second-nearest neighbor does not follow the shortest possible path along the cubic lattice, it is due to an obstacle or entanglement.

In Figure 1 the scheme used to compute the number of entanglements is illustrated for a square 2D lattice. The length of the path between second-nearest neighbors, beads "1" and "3", and "2" and "4" cannot be any shorter. However, the length of the path between beads "3" and "5" is longer than the shortest possible path, denoted by the dashed line of length $\sqrt{2}$. To avoid double-counting the same entanglement, we do not consider the second-nearest neighbors "4" and "6" and instead proceed to evaluate the distance between the beads "5" and "7" and "6" and "8". Using this method, we claim that the chain in Figure 1 has two entanglements. The general algorithm to enumerate entanglements on a PP in two or three dimensions may be summarized as follows:

1. Initialize bead position counters, $i_1 = 1$, $i_2 = 2$, $i_3 = 3$, and the number of entanglements $Z = 0$.

2. Compute the length of the PP between beads i_1 and i_3, l_{pp}, and the shortest possible path between beads i_1 and i_3, along the lattice, l_{sh}.

3. If $l_{\mathrm{pp}} = l_{\mathrm{sh}}$, then increment the counters: $i_1 = i_1 + 1$, $i_2 = i_2 + 1$, and $i_3 = i_3 + 1$.

4. If $l_{\mathrm{pp}} > l_{\mathrm{sh}}$, then increment the number of entanglements, $Z = Z + 1$, and the counters, $i_1 = i_1 + 2$, $i_2 = i_2 + 2$, and $i_3 = i_3 + 2$.

5. Repeat steps 2−4 until $i_3 > N$, where N is the total number beads.

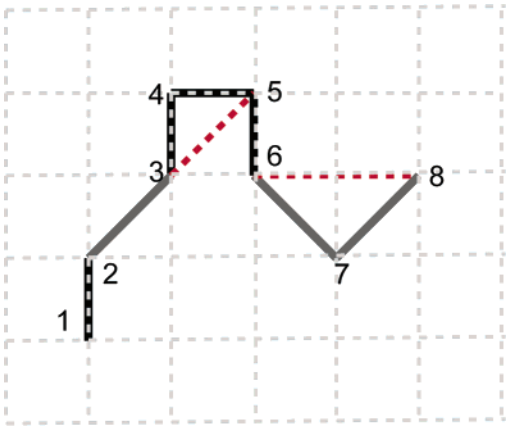

Figure 1. A 2D illustration of the algorithm used to compute the number of entanglements.

Table 1. Description of the Systems Simulated and Ensemble-Averaged Properties[a]

N	N_p	$\langle R^2 \rangle$	$\langle L_{pp} \rangle$	$\langle Z(\text{ens}) \rangle$	$\langle Z(\text{enum}) \rangle$
32	244	71.8 ± 3.8	11.0 ± 0.3	1.69 ± 0.11	0.85 ± 0.06
75	285	174.3 ± 8.0	23.2 ± 0.5	3.07 ± 0.17	2.22 ± 0.09
125	364	337.2 ± 14.6	37.3 ± 0.6	4.12 ± 0.20	4.12 ± 0.11
300	277	732.6 ± 36.9	85.5 ± 1.0	9.98 ± 0.53	9.61 ± 0.20
500	216	1189.3 ± 69.6	140.4 ± 1.5	16.57 ± 1.00	17.23 ± 0.32

[a] The last two columns show the number of entanglements evaluated by taking an ensemble average, $\langle Z(\text{ens}) \rangle = \langle L_{pp} \rangle^2 / \langle R^2 \rangle$, and by the enumeration algorithm. Equilibrating the $N = 125$ system required about 1.5 days, and annealing it to obtain L_{pp} required about 3 h on a single 1 GHz Pentium 3 processor.

Results and Discussion

We simulated linear chains with different number of beads, N, at a fractional density of $\phi = 0.5$ in a simulation box of size $L_{box} \times L_{box} \times L_{box}$ with periodic boundary conditions. The size of the box was chosen so that the number of chains in the ensemble is $N_p \approx 250$. First, we equilibrated the chains by the method described earlier and then annealed the system to obtain the PPs. A single Monte Carlo step involved $N \times N_p$ trial moves. In this paper, all distances are reported in units of lattice spacing. The simulation parameters, the resulting ensemble averages, the mean-squared end-to-end distances $\langle R^2 \rangle$, and the PP lengths $\langle L_{pp} \rangle$ are summarized in Table 1.

Additionally, the number of entanglements is calculated indirectly by using the formula from the tube model,[22] which computes the average number of entanglements Z(ens) per chain from the ensemble averages of the tube length squared $\langle L_{pp} \rangle^2$ and the squared end-to-end chain length $\langle R^2 \rangle$, using the assumption that the tube is a random walk, yielding $\langle Z(\text{ens}) \rangle = \langle L_{pp} \rangle^2 / \langle R^2 \rangle$ steps in the average PP. Table 1 reports the number of entanglements calculated by averaging over the ensemble $\langle Z(\text{ens}) \rangle$ and by using the direct algorithm for enumerating entanglements. From Figure 2 it can be seen that for well-entangled systems ($N \geq 125$ in Table 1) the two methods are statistically indistinguishable.

An advantage of the enumeration algorithm is that the spatial location of an individual entanglement can be identified. For example, in Figure 1, the nodes 4 and 7 are points of entanglement. Thus, the PP segment vectors $\mathbf{r}_{1,4}$, $\mathbf{r}_{4,7}$, and $\mathbf{r}_{7,8}$ can be identified. For the well-entangled systems, we examined the distribution of the PP segment lengths and found that the distributions were independent of N as expected (see Figure 3).

The average PP segment length inferred from ensemble averaging is $\langle a(\text{ens}) \rangle = \langle R^2 \rangle / \langle L_{pp} \rangle = 8.69 \pm 0.26$, while that computed from the distribution shown in Figure 3 from the enumeration method $\langle a(\text{enum}) \rangle = 6.77 \pm 0.07$, which is about 20% smaller. This difference probably reflects a limitation of the coarse-grained nature of the lattice model. However, the ratio $\langle a(\text{enum}) \rangle / \langle a(\text{ens}) \rangle = 0.78$ is independent of the length of the polymer chain. Thus, the PP has the characteristics of a random walk in that its mean-square end-to-end distance is linear in the length of the path and that the average step size of the PP is independent of its length. However, the PP has a broad, approximately exponential, distribution of step sizes (see Appendix A).

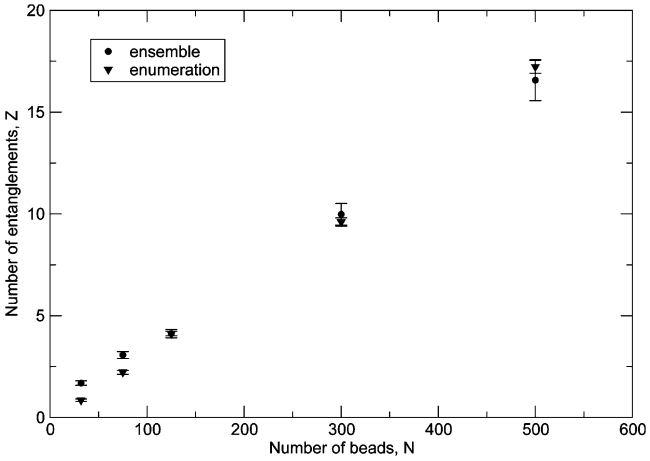

Figure 2. Number of entanglements from an ensemble average $\langle Z(\text{ens}) \rangle = \langle R^2 \rangle / \langle L_{pp} \rangle$ and from enumerating the entanglements, Z(enum), using the proposed algorithm, as a function of chain length.

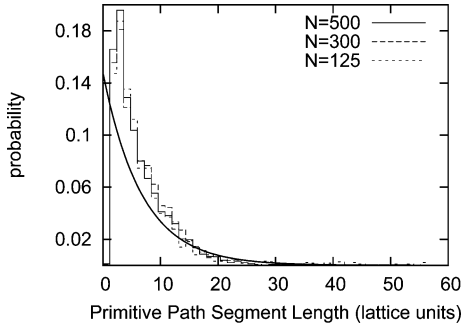

Figure 3. Distribution of PP segment lengths computed from the enumeration algorithm for well-entangled systems with $N \geq 125$. The distributions are essentially identical for all chain lengths as expected, with $\langle a \rangle = 6.77 \pm 0.07$. The solid line is the exponential distribution function $p(r) = \exp(-r/\langle a \rangle)/\langle a \rangle$.

Coupling of Entanglements in Concentrated Systems. As an application of this method of enumerating entanglements along a chain, we seek to estimate the number of additional entanglements released when a primitive chain i of Z_i entanglements is eliminated from the ensemble. This question provides a link between the dilution exponent α used in mean-field theories of polymer solutions and melts and the molecular-level question of how many chains on average are involved in an entanglement. Slip-link models,[23−26] which have been quite successful at describing a wide range of behavior of polymeric systems, often assume that entanglements arise out of binary contacts. This picture implicitly assumes $\alpha = 1$. On the other hand, Colby and Rubinstein[27] reported that for Θ-solvents $\alpha = 4/3$ is consistent with the assumption of a fixed number of binary contacts within an entanglement volume. Empirically, different sets of data support α values between 1 and 1.5.[28] A global fit of data reported in Tao et al. supports $\alpha = 1$.[28]

We consider a single replica of the PP network with $N = 300$ and $N_p = 277$, reported in Table 1. The number of

entanglements Z_i ($i = 1, 2, ..., N_p$) on all the chains was enumerated as described earlier, with $Z_{tot} = \sum_{i=1}^{i=N_p} Z_i$ and $\langle Z_i \rangle = Z_{tot}/N_p = 9.61 \pm 0.20$.

We select a primitive chain i from this system and delete it. The direct effect of this is to reduce the total number of entanglements in the system from Z_{tot} to $Z_{tot} - Z_i$. Further, the removal of chain i allows the geometrical constraints associated with it on the remaining $N_p - 1$ chains to disengage. We pull in this additional slack by quenching the system.[29] This step reduces the total number of entanglements in the ensemble by a further Z_i' to $(Z_{tot} - Z_i - Z_i')$.

After each of the $i = 1, ..., N_p$ chains has been selected for elimination with the other $N_p - 1$ chains retained, the dilution exponent α may be estimated as

$$\alpha = \left\langle \frac{Z_i'}{Z_i} \right\rangle \tag{3}$$

where $\langle [\cdot] \rangle \equiv 1/N_p \sum_i [\cdot]$. However, Z_i' obtained by the quenching routine depends on the order in which beads are considered for displacement. To mitigate this influence, we repeated the quenching process, each time with a different random order of bead displacements, $j = 1, 2, ..., m$ times. In general, $Z_i'(j = j_1) \neq Z_i'(j = j_2)$, for $j_1 \neq j_2$ (see Appendix B).

To calculate α, we concern ourselves with the maximum possible value of $Z_i'(j)$. This quantity Z_i^* is given by

$$Z_i^* = \lim_{m \to \infty} \{ \max_{j=1}^{m} Z_i'(j) \} \tag{4}$$

and thus eq 3 may be modified to

$$\alpha = \left\langle \frac{Z_i^*}{Z_i} \right\rangle \tag{5}$$

It is obviously infeasible to compute the exact limit implied in eq 4. To estimate Z_i^* using finite m, let us denote the maximum number of entanglements released in m trials by $Z_{i,max}^*(m)$, that is, $Z_{i,max}^*(m) = \max_{j=1}^{m} Z_i'(j)$. The value of "$\alpha$" estimated using m trials is therefore

$$\alpha_{est}(m) = \left\langle \frac{Z_{i,max}^*(m)}{Z_i} \right\rangle \tag{6}$$

Figure 4 shows the evolution of $\alpha_{est}(m)$ with m. As m increases, $d\alpha_{est}(m)/dm$ decreases (inset in Figure 4) according to the empirical expression

$$\frac{d\alpha_{est}}{dm} = \frac{0.1218}{m^{1.46}} \tag{7}$$

$\alpha_{est}(m = 50)$ approaches a value of 0.94 ± 0.02. However, as long as the slope $d\alpha_{est}(m)/dm$ is positive, $\alpha_{est}(m = 50)$ cannot be claimed as the asymptotic value, $\alpha_{est}(m \to \infty)$, and it merely provides a lower bound. Since $d\alpha_{est}(m)/dm$ decays faster than $1/m$, we can obtain the asymptotic value as

$$\alpha_{est}(m \to \infty) = \alpha_{est}(m = 1) + \int_1^{\infty} \frac{d\alpha_{est}}{dm} dm \tag{8}$$

Substituting eq 7, $\alpha_{est}(m \to \infty) = 0.77 + 0.26 = 1.03 \pm 0.02$.

Summary

In this article we propose a method to locate spatially an entanglement on any particular chain in a dense system of chains on a lattice by seeking local excursions of the PP from the shortest path connecting beads along the lattice. We validated this method by comparing it with the annealing algorithm developed earlier.[16] We examined the nature of coupling between entanglements using this algorithm and found that the lattice model supports a value of α that is closer to 1 than to 4/3. This is consistent with the description of entanglement junctions as binary contacts. When the dynamic dilution theory is used in conjunction with the higher dilution exponent of $\alpha = 4/3$,[30,31] it describes experimental data on branched polymer melts quantitatively. However, it may be noted that the slip-link model of Shanbhag et al.,[25] which implicitly assumes $\alpha = 1$, produces the same dilution effect as the dynamic dilution theory with $\alpha = 4/3$. Considering the empirical data compiled in Tao et al.,[28] where a global fit to all the available data, including that of Colby and Rubinstein yields $\alpha = 1$,[27] our lattice simulations suggest that the "true" value of α may differ from the value of α that works best with the dynamic dilution theory.

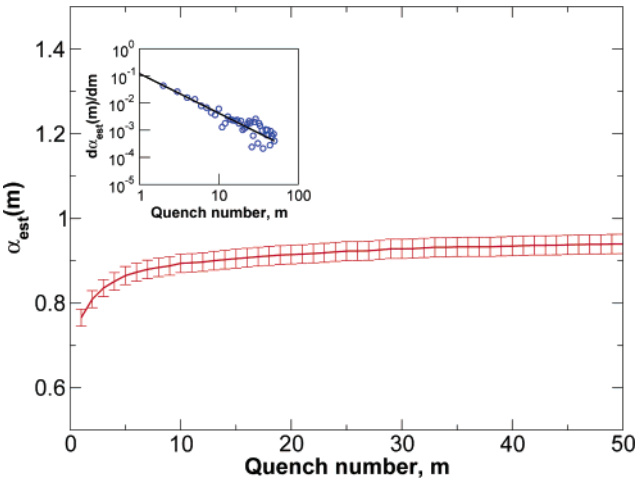

Figure 4. As the number of quenching trials m increases, $\alpha_{est}(m)$ given by eq 6 changes from $\alpha_{est}(m = 0) = 0.77 \pm 0.02$ to $\alpha_{est}(m = 50) = 0.94 \pm 0.02$. The inset shows the rate of increase of α_{est} with m on a log−log scale, and the straight line represents a power-law fit, $d\alpha_{est}/dm = 0.1218/m^{1.46}$. Based on this rate of increase, $\alpha_{est}(m)$ approaches an asymptotic value, $\alpha_{est}(m \to \infty) = 1.03 \pm 0.02$.

Acknowledgment. This material is based upon work supported by the National Science Foundation under Grant DMR 0305437. Any opinions expressed are those of the authors, not of NSF. The authors thank Qiang Zhou and Jay Schieber for helpful discussions and an anonymous referee for useful suggestions on improving the manuscript.

Appendix A. Distribution of Entanglements in the Primitive Path Network

The PP network obtained from the simulations is not a random walk consisting of a fixed number of equal step lengths. In fact, it is clear from Figure 3 it is clear that the PP step length has a fairly broad distribution.

Further, we investigated the entanglement network for the distribution of entanglements Z_i, over all the i chains in the ensemble for $N = 125$, 300, and 500 (see Figure 5). The distribution of entanglements per chain can be characterized by a Poisson distribution function

$$p(Z) = \frac{\lambda^Z \exp(-\lambda)}{Z!} \tag{9}$$

where the mean of the Poisson distribution $\lambda = \langle Z_i(N) \rangle$, as shown

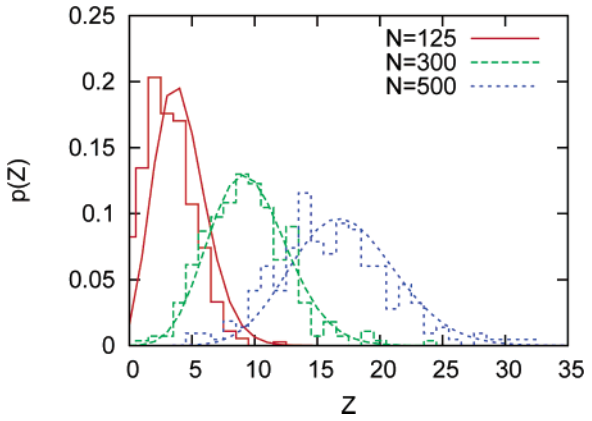

Figure 5. Histogram depicting the distribution of the number of entanglements Z_i over all the i chains in the ensemble for $N = 125$, 300, and 500. The solid curves are Poisson distributions, $p(Z) = \lambda^Z \exp(-\lambda)/Z!$ with $\lambda = \langle Z_i(N)\rangle = \langle Z(\text{enum})\rangle$ for each N from Table 1.

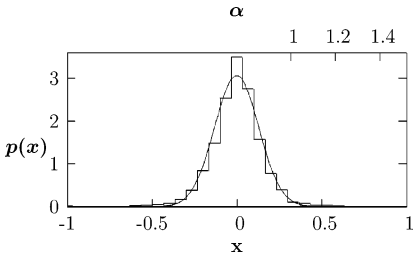

Figure 6. Distribution of x for the case of $N = 300$, renormalized so that the area under the histogram is unity. This distribution has been obtained from $N_p \times m = 13\,850$ different deviates. The dotted lines is the best-fit Gaussian distribution, $N(\mu = 0, \sigma = 0.13)$. The secondary x-axis on the top of the graph indicates the value of α corresponding to the choice of $x = x_{max}$ at the bottom of the graph.

by Figure 5. This is consistent with a process in which entanglements are created randomly along the length of the chain.

Appendix B. Distribution of Entanglements Lost after the Removal of a Chain

During the quenching trials, the number of entanglements lost after the removal of chain i, Z_i', varies. In general, for two different quenching operations, j_1 and j_2, $Z_i'(j_1) \neq Z_i'(j_2)$.

To assess the breadth of the distribution of $Z_i'(j)$ with respect to the mean Z_i', let us define a normalized variable

$$x(i,j) = \frac{Z_i'(j)}{\bar{Z}_i'} - 1 \qquad (10)$$

where $\bar{Z}_i' = \sum_{j=1}^{m} Z_i'(j)/m$ is the mean number of entanglements lost by the removal of chain i over m quenching trials.

For the case of $N = 300$, we obtained $N_p \times m = 277 \times 50 = 13\,850$ different measures of x. A histogram of these values is shown in Figure 6. It may be observed that the distribution of x is approximately Gaussian ($N(\mu = 0, \sigma = 0.13)$) and is sharply peaked at $x = 0$, as expected. From eq 5 in the text, $\alpha = \langle Z_i^*/Z_i\rangle$. If we set an upper bound x_{max} on the right wing of x corresponding to Z_i^*, then $1 + x_{max} = Z_i^*/\bar{Z}_i'$. Therefore, $\alpha = \langle Z_i^*/Z_i\rangle = (1 + x_{max})\langle \bar{Z}_i'/Z_i\rangle$. From the simulation, $\langle \bar{Z}_i'/Z_i\rangle = 0.76 \pm 0.02$, which requires $x_{max} = 0.36$ for $\alpha = 1.03 \pm 0.02$. This value of x_{max} corresponds to 2.76 standard deviations from the mean of the Gaussian distribution. Values of $x > x_{max}$ correspond to rare chains whose removal is able to induce loss of more than the typical number of entanglements on other chains.

Note Added after ASAP Publication. This article was published ASAP on February 7, 2006. Changes have been made to refs 21 and 25. The correct version was posted on February 9, 2006.

References and Notes

(1) Kremer, K.; Grest, G.; Carmesin, I. *Comput. Phys. Commun.* **1988**, *61*, 566−569.
(2) Kremer, K.; Grest, G. *J. Chem. Phys.* **1990**, *92*, 5057−5086.
(3) Ben-Naim, E.; Grest, G.; Witten, T.; Baljon, A. *Phys. Rev. E* **1996**, *53*, 1816−1822.
(4) Pütz, M.; Kremer, K.; Grest, G. S. *Europhys. Lett.* **2000**, *49*, 735−741.
(5) Everaers, R.; Kremer, K. *Phys. Rev. E* **1996**, *53*, R37.
(6) Everaers, R.; Sukumaran, S.; Grest, G.; Svaneborg, C.; Sivasubramanian, A.; Kremer, K. *Science* **2004**, *303*, 823−826.
(7) Sukumaran, S.; Grest, G.; Kremer, K.; Everaers, R. *J. Polym. Sci., Polym. Phys.* **2005**, *43*, 917−933.
(8) Auhl, R.; Everaers, R.; Grest, G. S.; Kremer, K.; Plimpton, S. J. *J. Chem. Phys.* **2003**, *119*, 12718−12728.
(9) Carmesin, I.; Kremer, K. *Macromolecules* **1988**, *21*, 2819−2823.
(10) Shaffer, J. *J. Chem. Phys.* **1994**, *101*, 4205−4213.
(11) Shaffer, J. *J. Chem. Phys.* **1995**, *103*, 761−772.
(12) Shaffer, J. *Macromolecules* **1996**, *29*, 1010−1013.
(13) Szamel, G.; Wang, T. *J. Chem. Phys.* **1997**, *107*, 93−98.
(14) Brown, S.; Szamel, G. *Macromol. Theory Simul.* **2000**, *9*, 14−19.
(15) De Cecca, A.; Freire, J. *Polymer* **2003**, *44*, 2589−2597.
(16) Shanbhag, S.; Larson, R. *Phys. Rev. Lett.* **2005**, *94*, 076001.
(17) In a strict sense, there are no topological obstacles in a system of linear chains since, given sufficient time, a chain can diffuse and release all topological restrictions. Henceforth, in this paper, we use the label "topological constraint" or "obstacle" to denote the spatial restriction on the motion of a test chain due to surrounding chains at time scales small than the reptation time of the chain.
(18) Kröger, M. *Comput. Phys. Commun.* **2005**, *168*, 209−232.
(19) Binder, K.; Paul, W. *J. Polym. Sci., Polym. Phys.* **1997**, *35*, 1−31.
(20) Zhou, Q.; Larson, R. *Macromolecules* **2005**, *38*, 5761−5765.
(21) Kröger, M. *Phys. Rep.* **2004**, *390*, 453−551.
(22) Doi, M.; Edwards, S. F. *The Theory of Polymer Dynamics;* Clarendon Press: Oxford, 1988.
(23) Hua, C.; Schieber, J. *J. Chem. Phys.* **1998**, *109*, 10018−10027.
(24) Doi, M.; Takimoto, J. *Philos. Trans. R. Soc. London, Ser. A* **2003**, *361*, 641−650.
(25) Shanbhag, S.; Larson, R.; Takimoto, J.; Doi, M. *Phys. Rev. Lett.* **2001**, *87*, 195502.
(26) Masubuchi, Y.; Takimoto, J.; Koyama, K.; Ianniruberto, G.; Marrucci, G.; Greco, F. *J. Chem. Phys.* **2001**, *115*, 4387−4394.
(27) Colby, R.; Rubinstein, M. *Macromolecules* **1990**, *23*, 2573−2757.
(28) Tao, H.; Huang, C.; Lodge, T. *Macromolecules* **1999**, *32*, 1212−1217.
(29) After removal of chain i from the primitive network, if we attempt to rope in the extra slack by repeating the standard annealing procedure on the $N_p - 1$ chains via eq 1, instead of quenching, the primitive chain network loses its structural resemblance to the original network. For example, it is possible that the number of entanglements on some of the remaining chains in the system actually increases, after the annealing operation. This makes it hard to assign direct meaning to the additional entanglements lost, Z_i'.
(30) Ball, R.; Mcleish, T. *Macromolecules* **1989**, *22*, 1911−1913.
(31) Milner, S.; McLeish, T. *Macromolecules* **1997**, *30*, 2159−2166.

MA052317V